ESTIMATION OF CERCHAR ABRASIVITY INDEX OF ANDESITIC ROCKS IN ECUADOR FROM CHEMICAL COMPOUNDS AND PETROGRAPHICAL PROPERTIES USING REGRESSION ANALYSES

F. Javier Torrijo[a,*], Julio Garzón-Roca[a], Julio Company[a], Guillermo Cobos[a]

[a] Department of Geotechnical Engineering, Universitat Politècnica de València, Camino de Vera s/n, 46022, Valencia, Spain.

[*]*Corresponding author*. Tel.: +34 963 877 582; fax: +34 963 877 569; E-mail address: fratorec@trr.upv.es

Abstract

An important issue in any rock engineering project is the adequate prediction of tool consumption. Excavation tools are subjected to wear and repair/replacement of those tools is usually an important expense on any excavation budget. The key factor that affects wear of excavation tools is rock abrasivity. In mining and civil engineering, rock abrasivity is typically measured by the Cerchar Abrasivity Index (*CAI*), which is obtained in laboratory from a Cerchar abrasivity test. This paper studied the relation between *CAI* and the chemical compounds and petrographical properties of andesitic rocks coming from the central area of Ecuador. A series of regression analyses are performed to study the influence of the different chemical compounds and petrographical properties on the *CAI* value. Results show that it is possible to make a good estimation of *CAI* from the plagioclase grain size and/or the content in SiO_2, FeO, MgO, CaO, Na_2O and K_2O compounds.

Keywords: Cerchar Abrasivity Index; andesitic rock; chemical compounds; petrographical properties.

1. Introduction

Material tool consumption is one of the main indicators of rock excavation in mining and civil engineering projects (e.g. tunnelling, underground mining and quarrying). In fact, an important issue in any rock project is the adequate prediction of tool consumption, being especially during the tendering stage a significant factor in the estimation of expenses. Either rock excavation is performed by conventional drilling and blasting or by means of mechanized excavators such as TBMs, roadheaders and dozers, excavation tools are exposed to wearing. Although wear partially depends on the machinery being used for excavation and the geological conditions, the key factor that affects wear of excavation (cutting) tools is rock abrasivity. Repair and replacement of rock cutting tools as well as other machine components in contact with the rock during excavation (which are also subjected to wear) have been reported to be an important amount on any excavation budget (Fowell and Abu Baker, 2007; Hamzaban et al., 2014b). Hence rock abrasivity is a very important factor to consider in the operating costs and performance of any mechanical rock excavation work. It should also be noted that mechanical rock excavation is usually carried out by machines of high cost and in most cases site specific, thus selecting the adequate cutter tool according to the rock abrasivity to be excavated is essential when looking for an optimum performance.

The abrasivity of rocks can be related to their petrographic composition, especially with the amount of hard minerals like quartz (Käsling and Tara, 2010), but other features such as the mean grain size, type of cement, and degree of cementation can influence the abrasivity of a rock (West, 1989; Yarali et al., 2008). Petrological methods may be used to estimate abrasivity (West, 1989). That includes Mohs's scratch hardness, Vickers hardness, silica content or microscopic examination of a thin section. Mechanical parameters such as uniaxial compression strength, tensile strength and fracture toughness may also be taken into account (Alber, 2008; Deliormanlı, 2012). However, typically abrasivity of rocks is more technically obtained from laboratory tests and associated with some kind of model or an index. Nowadays, Cerchar abrasivity test (CERCHAR, 1986; ASTM-

D7625, 2010; Alber et al., 2014) is probably the most common tests used to evaluate abrasivity of rocks, especially in the area of civil engineering (tunnelling), thanks to its simplicity and dependable results (Atkinson et al., 1986a, 1986b). From this test, the Cerchar Abrasivity Index (*CAI*) is obtained and used as the parameter which describes the abrasivity of rocks. Both the test and how to obtain that index will be explained later in this paper.

Several researches studied the dominant factors of *CAI* (Rostami et al., 2014) and the effects that different aspects can have on *CAI*, such as quartz content, grain size and matrix properties (Suana and Peters, 1982; Lassnig et al., 2008), rock strength (Al-Ameen and Wallner, 1994) stress dependency (Alber, 2007) or testing conditions, procedures and materials used to conduct the test (Al-Ameen and Wallner, 1994; Plinninger et al., 2003; Michalakopoulos et al., 2005; Fowell and Abu Bakar, 2007; Lassnig et al., 2008; Hamzaban et al., 2014a; Rostami et al., 2014). Likewise, some investigations analysed and correlate *CAI* with mechanical and/or geological properties, including chemical compounds, petrographical properties, equivalent quartz content, uniaxial compression strength or Young modulus (Plinninger et al., 2003; Kahraman et al., 2010; Deliormanlı, 2011; Moradizadeh et al., 2013; Er and Tugrul, 2016a, 2016b; Majeed and Bakar, 2016). Nevertheless, most of the mentioned studies only dealt with some rock specific samples (e.g. granitic rocks), and up to now there is not a clear evidence that their results may be completely extrapolated and used when facing other rock formations.

In this paper a relation between *CAI* and the chemical compounds and petrographical properties of andesitic rocks is investigated. A total of 73 andesitic samples coming from the central area of Ecuador are subjecting to Cerchar abrasivity tests and are chemically and petrographically analysed, in order to establish both *CAI* and their chemical and modal compounds as well as minerals grain size. A series of regression analyses are performed studying the influence of the different chemical compounds and petrographical properties on *CAI* value. Regression analyses are frequently used in engineering and have recently demonstrated to be effective to correlate *CAI* with mechanical and geological properties (Er and Tugrul, 2016a, 2016b; Majeed and Bakar, 2016). Both simple regression and multiregression models are considered in this paper.

2. Geographical Setting and Geological Framework

The andesite samples analysed in this study come from the Bombolí area (Mejía canton, Pichincha province, Ecuador), where the construction of a new road tunnel is currently being built. The ca. 2 kilometer-long Bombolí tunnel runs between the kilometric points (kp) 20+221 and 21+959 of the E-20 road Alóag-Santo Domingo, approximately 50 Km South-West of the city of Quito (**Fig. 1**). The road Alóag-Santo Domingo stretches over mafic lavas and volcano-sedimentary rocks of the Western Cordillera of Ecuador, a north-south trending chain which is one of the two major branches of the Ecuadorian Andean Mountain Range (Vallejo, 2007; Vallejo et al., 2009; Vera, 2016).

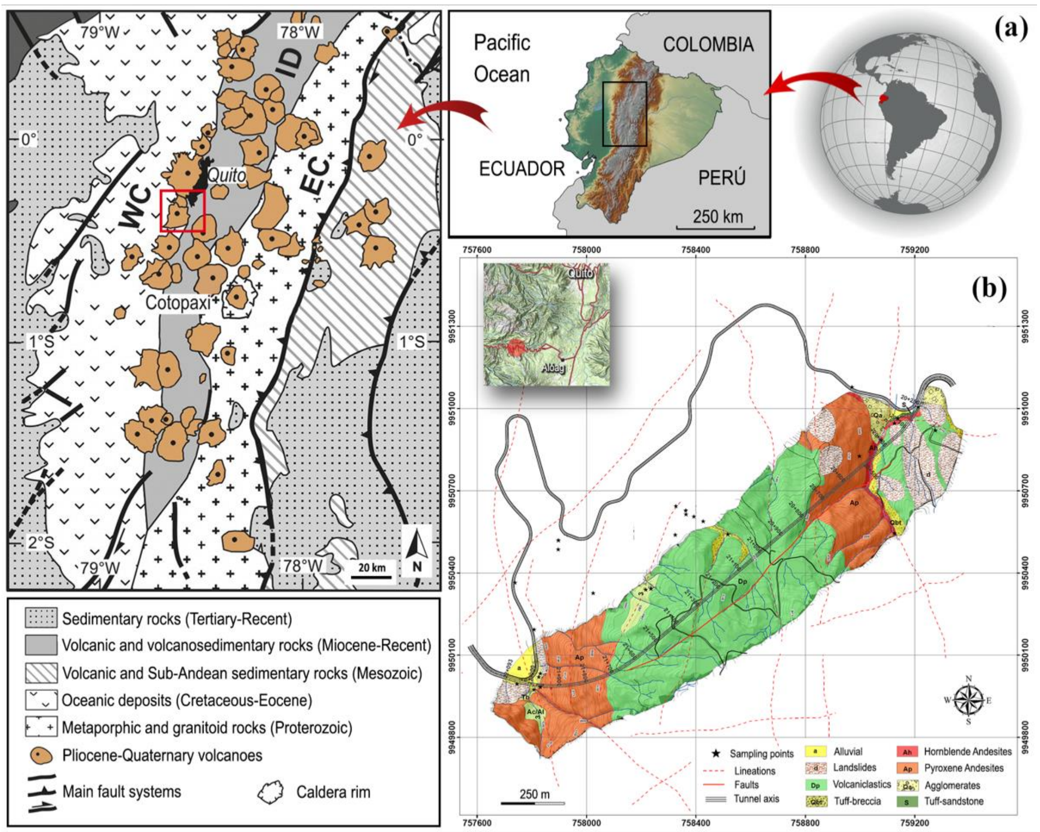

Fig. 1. Sketch maps showing the location of the studied area. The successive insets show the position of the detailed maps: a) Geological simplified map of the Ecuadorian Andes showing the main stratigraphic units outcropping in the region. (Modified from Vezzoli et al. 2017). Abbreviations: EC = Eastern Cordillera; ID = Interandean Depression; WC = Western Cordillera; b) Detailed map of the Bombolí road tunnel showing the different volcano-sedimentary materials affected by mechanical rock excavations and sample locations.

In the project area, the extensive exposures of volcano-sedimentary materials can be mainly referred to the Silante Formation, an upper Maastrichtian-Paleocene volcanic unit whose type section crops out along the Alóag–Santo Domingo road. The Silante Formation consists (**Fig. 2**) of a thick succession of andesitic volcaniclastic deposits (fluvial conglomerates and Breccias, mudstones, siltstones and tuffaceous sandstones) with intercalations of andesites, dacites and breccias (Boland et al., 2000).

Fig. 2. View of the andesitic rocks studied in the project area.

3. Experimental study

Up to 73 andesitic rock samples from the project area were selected for mechanical and petrographic analyses. Samples were extracted from three locations along the Bombolí area: 27 samples belonged to inside of tunnel, and will refer thereafter as TB; 16 samples were obtained from the slopes, TT samples thereafter; and 30 samples corresponded to the road, refer as VC thereafter.

3.1. XRF analysis

The main chemical compounds of the andesitic samples were identified by a semi-quantitative chemical analysis with X-ray fluorescence spectroscopy, carried out using a Perkin-Elmer 3030.

3.2. Petrographical characteristics

Thin sections were prepared for the 73 andesitic rock samples and studied under a petrographic polarizing microscope for determining grain size and quantitative mineral content.

3.3. Physical and mechanical properties and Cerchar abrasivity index

Several tests were conducted on each group of samples to set their physical and mechanical properties. Those tests included determining the unit weight and obtaining the uniaxial compression strength and the tensile strength of the intact rock. Tests were conducted based on ISRM (2007) and ASTM standards (ASTM D7012; ASTM D3967).

The 73 andesitic rock samples were subjected to Cerchar abrasivity tests. This test, introduced in the 1970s by the Centre d'Etudes et Recherches des Charbonages de France (CERCHAR) for assessing abrasivity in the coal mining industry (Yarali et al., 2008; Kasling and Thuro, 2010), was later adopted by the tunnelling industry (West, 1989; Rostami et al., 2014), and is nowadays typically selected as a tool to quantify rock abrasivity in predicting tool wear during hard rock tunnelling. Cerchar abrasivity test (**Fig. 3**) measures the wear on the tip of a steel stylus having a Rockwell Hardness of HRC 55. Two standards exist for this test method: the French standard NF P 94-430-1 (2000) and ASTM D7625-10 (2010). The test presented in this paper followed the former and ISRM suggested method (Alber et al., 2014), as well as the original specifications of the test (CERCHAR, 1986). To measure the wear flat of the Cerchar test stylus, side view method was used, since that introduces less statistically significant error in the measured values of *CAI*. The stylus scratches the surface of a rough rock sample over a distance of 10 mm under static load of 70

N. The wear surface of the stylus tip is afterwards measured under a microscope to an accuracy of 0.01 mm. The wear surface, stated in units of 0.01 mm, is then multiplied by 10 to obtain the Cerchar Abrasivity Index (*CAI*), which is a dimensionless unit value. The test is performed at least five times on the same rock surface by using a fresh re-sharpened stylus each time and then taking the arithmetic mean of the measured values.

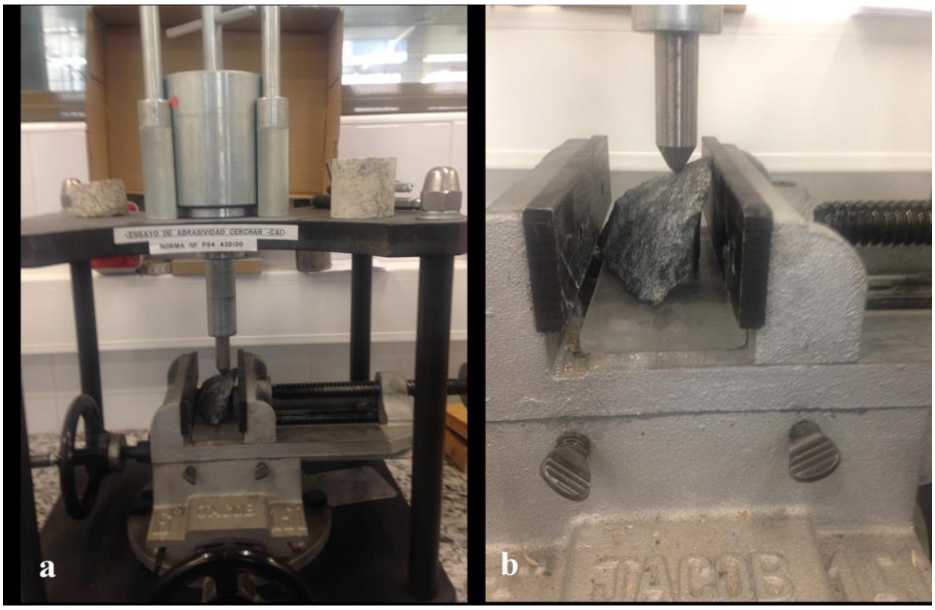

Fig. 3. Cerchar abrasivity test conducted: a) Cerchar device; b) Detail of the rock sample and the steel stylus.

The French standard AFNOR NF P 94-430-1 (2000) was follow. Tests were performed at the laboratories of the Department of Geotechnical Engineering of the Technical University of Valencia, by one technician. The tip of a steel stylus had a Rockwell Hardness of HRC 55.

4. Results

4.1. XRF analysis

The andesitic samples under study are mainly composed (**Table 1**) of SiO_2, which represent ca. 50% or more in nearly all cases. The second more abundant compound is Al_2O_3, with ca. 15%, followed by the CaO, with ca. 10%. Other compounds such as Fe_2O_3, FeO, MgO, Na_2O, K_2O appear in small quantities (between 2% and 10% on average) and some traces of TiO_2, MnO, P_2O_5 are also found in the samples.

Table 1. Chemical compounds of andesitic samples.

Sample	Chemical compounds (%)									
	SiO_2	TiO_2	Al_2O_3	Fe_2O_3	FeO	MnO	MgO	CaO	Na_2O	K_2O	P_2O_5
TB1	55.21	0.88	16.35	5.53	4.09	0.15	3.36	9.06	3.53	1.64	0.20
TB2	61.33	0.89	10.98	2.39	3.98	0.19	3.40	11.51	3.25	1.88	0.20
TB3	64.16	0.90	11.22	1.79	3.87	0.23	3.44	9.10	2.97	2.12	0.20
TB4	55.30	0.91	16.29	1.87	3.76	0.27	3.48	12.87	2.69	2.36	0.20
TB5	60.72	0.92	6.90	2.93	3.65	0.31	3.52	15.84	2.41	2.60	0.20
TB6	54.20	0.93	17.59	6.32	3.54	0.35	3.56	8.34	2.13	2.84	0.20
TB7	55.01	0.94	17.90	4.98	3.43	0.39	3.60	8.62	1.85	3.08	0.20
TB8	65.10	0.95	11.03	1.62	3.32	0.43	3.64	8.82	1.57	3.32	0.20
TB9	66.00	0.96	13.28	2.22	3.21	0.47	3.68	5.13	1.29	3.56	0.20
TB10	60.76	0.60	13.81	4.06	8.27	0.90	2.31	4.14	3.53	1.42	0.19
TB11	58.91	1.03	15.38	1.82	2.46	0.34	2.54	12.00	3.25	2.07	0.19
TB12	59.16	0.58	14.86	3.73	8.65	1.10	2.20	4.43	2.99	2.12	0.19
TB13	56.30	0.57	16.64	5.19	8.84	1.25	2.15	5.41	2.69	0.76	0.19
TB14	57.15	0.56	15.76	4.19	3.03	1.41	2.09	8.71	2.52	4.39	0.19
TB15	55.90	0.54	17.20	4.11	8.15	1.42	2.04	5.06	2.42	2.96	0.19
TB16	58.12	0.53	12.79	4.69	9.41	1.73	1.98	3.81	1.85	5.00	0.08
TB17	53.31	0.52	17.13	4.52	9.60	1.26	1.93	8.73	1.57	1.24	0.19
TB18	54.70	0.51	14.55	4.45	4.79	2.04	1.87	14.93	1.29	0.67	0.19
TB19	45.92	0.48	18.43	5.86	9.98	2.20	1.82	8.27	3.53	3.32	0.19
TB20	53.08	0.48	9.63	4.56	10.17	2.35	1.77	11.02	3.25	3.56	0.13
TB21	62.43	0.83	17.62	5.78	6.86	0.35	1.71	0.11	2.69	1.42	0.19
TB22	56.54	0.46	16.15	3.94	10.55	0.39	1.66	5.65	2.41	2.07	0.19
TB23	50.31	0.45	17.15	4.49	10.74	0.43	1.60	10.39	2.13	2.12	0.19
TB24	45.92	0.43	19.37	5.86	5.35	0.47	1.55	18.24	1.85	0.76	0.19
TB25	75.00	0.42	2.98	1.55	1.27	0.90	1.49	10.23	1.57	4.39	0.19
TB26	61.62	0.41	14.61	3.01	1.09	0.94	1.44	10.19	3.53	2.96	0.19
TB27	53.31	0.40	16.29	4.52	0.57	2.04	1.39	16.17	3.25	1.88	0.19
TT1	51.46	0.39	14.32	4.86	11.69	2.20	1.33	8.75	2.69	2.12	0.19
TT2	53.77	1.16	16.05	5.40	2.77	2.35	4.48	10.65	2.41	0.76	0.20
TT3	59.08	1.17	15.38	3.48	1.31	0.35	4.52	8.00	2.13	4.39	0.20
TT4	55.85	1.18	16.35	5.02	2.31	0.39	4.56	10.73	0.45	2.96	0.20
TT5	60.23	1.19	15.03	3.27	0.68	0.43	4.60	9.48	0.17	4.80	0.12
TT6	54.46	1.20	16.78	4.31	0.57	1.43	4.64	11.45	3.53	1.42	0.20
TT7	69.46	1.21	9.90	1.90	0.46	0.03	4.65	6.87	3.25	2.07	0.20
TT8	43.38	1.22	20.14	7.29	0.35	1.51	4.72	16.10	2.97	2.12	0.20
TT9	60.23	0.97	15.02	3.15	4.15	0.51	3.72	8.29	3.00	0.76	0.20
TT10	53.08	0.98	17.20	4.56	2.99	0.55	3.12	9.73	3.20	4.39	0.20
TT11	55.85	0.99	16.36	5.02	2.05	0.59	3.80	9.58	2.60	2.96	0.20
TT12	57.92	1.00	14.79	3.68	4.81	0.63	3.84	11.08	0.17	1.88	0.20
TT13	53.54	0.90	17.06	4.48	4.09	0.15	3.36	10.58	3.53	2.12	0.19
TT14	54.46	0.81	16.78	5.28	3.98	0.19	3.40	9.77	3.25	1.98	0.10
TT15	54.92	0.90	16.64	4.23	3.87	0.23	3.44	10.48	2.97	2.12	0.20
TT16	52.15	1.01	16.62	4.73	5.66	0.67	3.88	11.42	3.00	0.76	0.09
VC1	50.54	1.05	17.97	4.45	2.22	0.83	4.04	11.21	3.20	4.39	0.10
VC2	51.00	0.86	14.44	4.94	2.11	0.87	4.08	15.95	2.60	2.96	0.19
VC3	56.77	1.02	16.08	2.30	2.55	0.71	3.92	8.34	2.99	5.00	0.32
VC4	53.54	1.03	17.05	4.48	2.50	0.75	3.96	11.98	3.27	1.24	0.20
VC5	59.31	0.89	15.31	4.40	3.99	0.35	3.56	5.85	5.50	0.67	0.19
VC6	55.62	0.87	15.49	3.77	4.16	0.29	3.50	9.80	6.10	0.21	0.19
VC7	47.54	0.86	17.95	5.57	4.33	0.24	3.45	13.43	4.57	1.88	0.19
VC8	54.46	0.84	15.95	3.92	4.50	0.19	3.08	7.45	7.29	2.12	0.19
VC9	52.85	0.82	17.27	4.61	4.67	0.14	3.35	7.46	7.89	0.76	0.19
VC10	54.69	0.81	15.77	4.27	4.15	0.09	3.30	6.07	6.28	4.39	0.19
VC11	52.15	0.79	17.48	4.24	5.01	0.03	3.24	9.87	4.04	2.96	0.19
VC12	54.00	0.78	16.91	5.36	5.18	0.02	3.19	7.28	2.10	5.00	0.19
VC13	54.46	1.63	16.78	3.92	2.33	0.79	4.00	11.34	3.12	1.42	0.20
VC14	50.31	0.81	17.15	1.65	5.05	0.02	3.23	10.56	8.95	2.07	0.19
VC15	56.54	0.80	16.15	3.94	5.24	0.32	3.18	6.48	5.04	2.12	0.19
VC16	56.08	0.79	15.35	2.14	5.43	0.20	3.13	6.67	9.24	0.79	0.19
VC17	54.00	0.78	16.92	3.99	5.62	0.19	3.07	7.78	3.28	4.19	0.19
VC18	59.08	0.77	12.45	3.48	5.81	0.19	3.02	7.60	4.46	2.96	0.19
VC19	53.08	0.75	17.20	4.56	6.00	0.19	2.96	7.60	6.17	1.30	0.19
VC20	52.85	0.74	16.42	5.57	6.19	0.19	2.91	7.43	6.46	1.05	0.20
VC21	50.31	0.73	18.04	1.36	6.38	0.91	2.85	12.40	5.85	0.98	0.20
VC22	51.00	0.71	17.83	1.87	6.57	0.92	2.80	14.10	2.99	1.02	0.19
VC23	54.00	0.70	16.09	4.40	6.76	0.93	2.74	9.28	3.27	1.64	0.19
VC24	45.92	0.84	18.42	5.86	6.95	0.94	2.69	14.31	2.99	0.89	0.19
VC25	51.23	0.68	16.89	5.86	7.13	0.24	2.64	11.00	3.27	0.87	0.19
VC26	46.85	0.67	19.09	5.70	7.32	0.19	2.58	11.06	5.50	0.86	0.19
VC27	52.38	0.65	17.41	4.69	7.51	0.14	2.53	7.54	6.10	0.84	0.20
VC28	54.23	0.64	16.02	4.35	7.70	0.09	2.47	8.90	4.57	0.82	0.19
VC29	54.46	0.63	16.78	5.28	7.89	0.03	2.42	4.26	7.29	0.76	0.19
VC30	59.31	0.62	15.31	3.43	8.08	0.15	2.36	2.58	3.58	4.39	0.18

4.2. Petrographical characteristics

The studied samples exhibit variability in crystallinity and in mineralogical composition but, in general, can be characterized as subvolcanic andesitic porphyrites. Plagioclase and clinopyroxene are the main minerals in all samples analysed, showing variations in their mineral contents (**Table 2**) and grain sizes (**Table 3**). The equivalent quartz content (EQC) was determined according to Thuro (1997). A suggested equation is shown in Eq. 1:

$$EQC = \sum A_i \cdot R_i \qquad (1)$$

where A_i is the mineral amount (%) and R_i is the Rosiwal abrasiveness value for each mineral, respectively.

In hand specimens, the Bombolí tunnel andesites exhibit a seriate porphyritic texture, with visible phenocryst of plagioclases surrounded by a greenish grey fine-grained matrix. Polished thin sections show largely euhedral to subhedral plagioclase phenocrysts, scanty subhedral clinopyroxenes (between 5-13% of phenocrists) and occasional hornblende phenocrists, with opaques as accessory minerals (**Fig. 4**). Plagioclase crystals are generally unaltered and exhibit the characteristic lamellar twinning, even some phenocrysts are partially resorbed. Some of the plagioclase crystals show chemical zoning. Clinopyroxene phenocrystals are partially replaced by chlorite. Small microlites of plagioclase and clinopyroxenes are embedded in a dark, glassy groundmass.

4.3. Cerchar abrasivity index, physical and mechanical properties

Cerchar abrasivity index results obtained for each tested specimen are listed on **Table 3**. Unit weight of the studied intact rock was found to be 25.4 kN/m^3 for the TB samples, 24.9 kN/m^3 for the TT samples and 24.7 kN/m^3 for the VC samples. Regarding uniaxial compression strength, tests gave an average value of 35 MPa for the TB samples, 25 MPa for the TT samples and 30 MPa for the VC samples. Tensile strength was set to 10 MPa in the case of TB samples, 9 MPa in the case of TT samples and 8 MPa in the case of VC samples.

Table 2. Modal compounds of the studied andesitic samples.

Sample	Modal compounds (%)					EQC (%)
	Plagioclase	Clinopyroxene	Amphibole	Iron Ore	Cryptocrystalline material	
TB1	59.7	17.9	3.0	0.0	19.4	28.3
TB2	71.9	16.1	2.2	0.1	9.7	30.3
TB3	71.4	16.0	1.6	1.0	10.0	30.2
TB4	62.0	23.1	5.5	0.0	9.4	29.6
TB5	67.4	18.3	5.4	0.1	8.8	29.8
TB6	53.8	33.2	3.0	0.0	10.0	29.6
TB7	57.1	29.2	3.7	0.0	10.0	29.6
TB8	76.8	7.1	1.9	2.2	12.0	29.8
TB9	71.5	12.6	2.6	1.4	11.9	29.7
TB10	68.8	15.8	3.3	0.0	12.1	29.7
TB11	65.3	18.9	3.6	0.2	12.0	29.5
TB12	64.9	17.6	3.4	2.1	12.0	29.2
TB13	60.7	21.6	5.9	1.0	10.8	29.1
TB14	57.5	23.7	5.6	2.4	10.8	28.8
TB15	58.6	24.6	5.5	0.1	11.2	29.2
TB16	63.7	21.0	3.9	1.4	10.0	29.5
TB17	59.9	26.0	4.1	0.2	9.8	29.6
TB18	55.8	28.3	4.2	0.3	11.3	29.2
TB19	51.6	32.6	3.7	2.0	10.1	29.1
TB20	58.6	26.9	3.4	1.1	10.0	29.5
TB21	57.1	26.6	5.5	0.0	10.8	29.2
TB22	62.5	21.1	4.6	0.0	11.8	29.3
TB23	56.6	28.5	3.0	0.0	11.9	29.4
TB24	50.7	34.6	3.7	0.0	11.0	29.3
TB25	74.6	9.4	1.9	2.1	12.0	29.7
TB26	66.2	19.9	2.6	0.9	10.4	29.8
TB27	55.5	31.8	3.0	0.0	9.7	29.7
TT1	57.9	29.1	3.0	0.0	10.0	29.7
TT2	52.0	33.6	4.1	0.0	10.3	29.3
TT3	57.2	28.5	4.3	0.0	10.0	29.5
TT4	58.2	26.5	3.7	0.0	11.6	29.4
TT5	58.3	28.3	3.3	0.0	10.1	29.7
TT6	52.7	34.3	3.0	0.0	10.0	29.6
TT7	67.2	18.3	2.7	1.0	10.8	29.8
TT8	48.8	37.6	2.8	0.1	10.7	29.3
TT9	58.3	29.2	2.8	0.1	9.6	29.8
TT10	51.0	37.1	0.6	0.3	11.0	29.6
TT11	54.1	30.5	3.9	0.1	11.4	29.2
TT12	55.9	29.9	4.0	0.3	9.9	29.5
TT13	60.2	24.5	3.7	0.0	11.6	29.4
TT14	61.2	25.3	3.4	0.0	10.1	29.7
TT15	53.2	31.4	5.5	0.0	9.9	29.2
TT16	50.5	34.1	4.6	0.0	10.8	29.1
VC1	56.8	30.9	1.5	0.0	10.8	29.8
VC2	49.4	36.0	3.3	0.3	11.0	29.2
VC3	63.8	22.7	1.9	0.0	11.6	29.8
VC4	51.8	34.0	4.0	0.1	10.1	29.4
VC5	57.4	27.8	3.7	2.2	8.9	29.4
VC6	53.8	30.6	2.4	1.4	11.8	29.2
VC7	46.0	39.3	5.3	0.0	9.4	29.1
VC8	56.7	27.8	4.4	0.0	11.1	29.3
VC9	59.4	25.6	3.0	0.0	12.0	29.4
VC10	52.9	33.5	3.6	0.2	9.8	29.5
VC11	50.5	37.5	1.9	0.0	10.1	29.6
VC12	56.0	35.7	1.6	0.0	6.7	30.4
VC13	55.7	34.4	2.7	0.0	7.2	30.1
VC14	52.4	34.5	2.8	0.0	10.3	29.5
VC15	54.7	31.4	3.8	0.0	10.1	29.5
VC16	54.3	34.8	0.6	0.0	10.3	29.9
VC17	53.3	35.8	1.2	0.7	9.0	29.9
VC18	57.2	28.6	4.0	1.6	8.6	29.5
VC19	51.4	35.6	2.9	0.0	10.1	29.5
VC20	51.2	36.1	2.2	0.6	9.9	29.5
VC21	51.7	31.6	1.6	1.9	13.2	28.9
VC22	49.4	36.1	2.2	1.5	10.8	29.2
VC23	66.7	25.6	3.0	0.0	4.7	30.8
VC24	44.5	40.9	3.3	0.2	11.1	29.1
VC25	49.6	36.9	1.9	2.2	9.4	29.4
VC26	45.3	42.8	1.6	1.4	8.9	29.5
VC27	54.2	30.9	2.7	0.4	11.8	29.3
VC28	52.5	35.0	2.8	0.0	9.7	29.6
VC29	60.3	25.1	3.7	0.9	10.0	29.5
VC30	57.4	30.1	3.2	0.0	9.3	29.8

Table 3. Grain size and Cerchar abrasivity index (CAI).

Sample	Grain Size (mm)			CAI
	Plagioclase	Clinopyroxene	Amphibole	
TB1	1.04	0.64	0.87	2.30
TB2	1.20	0.80	0.61	2.82
TB3	1.33	0.33	0.66	3.02
TB4	1.07	0.58	0.87	2.43
TB5	1.08	0.48	0.45	2.69
TB6	0.80	0.45	0.53	2.11
TB7	0.90	1.00	0.62	2.20
TB8	1.37	0.66	0.33	3.10
TB9	1.30	0.46	0.27	2.86
TB10	1.20	0.67	0.62	2.65
TB11	1.11	0.63	0.87	2.56
TB12	1.13	0.31	0.45	2.50
TB13	1.03	1.10	0.53	2.38
TB14	0.99	0.34	0.33	2.39
TB15	0.96	0.70	0.27	2.30
TB16	1.24	0.90	0.61	2.50
TB17	1.04	0.30	0.66	2.31
TB18	0.89	0.50	0.71	2.19
TB19	0.85	0.32	0.43	1.99
TB20	1.00	0.18	0.36	2.30
TB21	1.06	0.68	0.29	2.24
TB22	1.15	0.43	0.27	2.45
TB23	0.93	0.19	0.62	2.18
TB24	0.83	0.20	0.83	1.99
TB25	1.33	0.46	0.29	3.25
TB26	1.21	0.78	0.72	2.67
TB27	0.92	0.50	0.75	2.31
TT1	1.00	0.36	0.76	2.23
TT2	1.26	0.57	0.18	2.33
TT3	1.11	0.43	0.20	2.56
TT4	1.22	0.56	0.45	2.42
TT5	1.22	0.70	0.33	2.61
TT6	1.04	0.30	0.22	2.36
TT7	1.33	0.48	0.27	3.01
TT8	0.93	0.17	0.23	1.88
TT9	1.18	0.20	0.56	2.61
TT10	1.01	0.34	0.76	2.30
TT11	1.18	0.60	0.39	2.42
TT12	1.09	0.55	0.42	2.51
TT13	1.03	0.55	0.87	2.32
TT14	1.05	0.57	0.76	2.36
TT15	1.07	0.59	0.37	2.38
TT16	0.89	0.44	0.75	2.26
VC1	0.98	0.21	0.38	2.19
VC2	1.04	0.12	0.57	2.21
VC3	1.06	0.15	0.76	2.46
VC4	1.05	0.18	0.36	2.32
VC5	1.17	0.34	0.65	2.57
VC6	1.03	0.71	0.44	2.41
VC7	0.96	0.68	0.36	2.06
VC8	1.01	0.41	0.32	2.36
VC9	1.08	0.69	0.29	2.29
VC10	1.07	0.76	0.17	2.37
VC11	1.02	0.63	0.62	2.26
VC12	1.06	0.65	0.67	2.34
VC13	1.07	0.75	0.61	2.36
VC14	0.98	0.64	0.46	2.18
VC15	1.11	0.56	0.36	2.45
VC16	1.10	1.20	0.29	2.43
VC17	1.06	0.21	0.27	2.34
VC18	1.16	0.34	0.62	2.56
VC19	1.04	0.54	0.77	2.30
VC20	1.03	0.43	0.56	2.29
VC21	0.98	0.53	0.59	2.18
VC22	1.00	0.67	0.61	2.21
VC23	1.06	0.78	0.58	2.34
VC24	0.91	0.45	0.19	1.99
VC25	1.02	0.56	0.27	2.22
VC26	0.93	0.34	0.45	2.03
VC27	1.02	0.58	0.23	2.27
VC28	1.06	0.63	0.15	2.35
VC29	1.09	0.76	0.38	2.36
VC30	1.15	0.64	0.23	2.57

Fig. 4. Representative photomicrograph in cross-polarized light of a porphyritic andesite sample from the project area (Bombolí hacienda, Ecuador) showing elongate, euhedral phenocrysts of plagioclase (grey interference colours, multiple twinning), clinopyroxene crystals (higher-order interference colours) and plagioclase microlites set in a glassy groundmass (black areas, optically isotropic). Clinopyroxene phenocrysts are partially altered and replaced by chlorite. Abbreviations: pl, plagioclase; cpx, clinopyroxene. Scale bar = 1 mm.

4.4. Statistical summary of the results

Table 4 shows a statistical summary of the results obtained. Average, standard deviation, coefficient of variation and minimum and maximum values are listed for the chemical compounds and the petrographical properties of the andesitic samples studied, as well as for the Cerchar Abrasivity Index (*CAI*). As may be observed, *CAI* shows little variation, with a coefficient of variation of about a 10%, while in general chemical compounds and petrographical properties exhibit more variability (with a coefficient of variation larger than a 50% in some cases).

Regarding the relation between the *CAI* and the grain size, if the test is scratch 10 mm, it turns out that on average: (i) 57.4% will be plagioclase crystals with an average size of 1.07 mm; (ii) 28.3% will be pyroxene crystals with an average size of 0.52 mm; (iii) 3.3% amphibole crystals with average size of 0.49 mm; (iv) 0.5% iron that we do not know its size or is rather dispersed; (v) 10.5% matrix. Hence, there is about 30% chance of scratching amphiboles and clinopyroxenes, approximately 60% of plagioclase and 10% of matrix, which is obvious from the distribution of minerals in the thin sections.

Table 4.Statistical summary.

	Average	Standard deviation	Coefficient of variation (%)	Minimum value	Maximum value
Chemical compounds (%)					
SiO_2	55.39	5.29	9.55	43.38	75.00
TiO_2	0.81	0.24	29.63	0.39	1.63
Al_2O_3	15.68	2.75	17.54	2.98	11.14
Fe_2O_3	4.12	1.32	32.04	1.36	7.29
FeO	4.98	2.76	55.42	0.35	11.69
MnO	0.65	0.62	95.38	0.02	2.35
MgO	3.03	0.91	30.03	1.33	4.72
CaO	9.39	3.36	35.78	0.11	18.24
Na_2O	3.49	1.86	53.30	0.17	9.24
K_2O	2.26	1.31	57.96	0.21	5.00
P_2O_5	0.19	0.03	15.79	0.08	0.32
Modal compounds (%)					
Plagioclase	57.44	6.80	11.84	44.50	76.80
Clinopyroxene	28.33	7.48	26.40	7.10	42.80
Amphibole	3.26	1.19	36.50	0.60	5.90
Iron Ore	0.49	0.73	148.97	0.00	2.40
Cryptocrystalline material	10.47	1.67	15.95	4.70	19.40
EQC (%)	29.51	0.36	1.22	28.30	30.80
Grain size					
Plagioclase	1.07	0.12	11.21	0.80	1.37
Clinopyroxene	0.52	0.22	42.31	0.12	1.20
Amphibole	0.49	0.21	42.86	0.15	0.87
CAI	2.39	0.25	10.46	1.88	3.25

Additionally, **Table 5** displays the correlation matrix between *CAI*, minerals and EQC. From the observation of this matrix, it follows that the *CAI* values with the plagioclase are logical in content and size of the crystal. Also with amphibole, but it does not have seemingly sense the variation that the clinopiroxeno presents. However, although the value of the correlation coefficient (0.78) is low, the most significant is the negative sign. This indicates that the greater existence of clinopyroxene lower *CAI*.

5. Analysis and Discussion

Regression analyses were conducted to study the influence of the different chemical compounds and petrographical properties of the andesitic samples on *CAI*. The statistical software STATGRAPHICS Centurion XVI v16.2.04 (StatPoint Technologies, 2009) was used to perform the statistical analyses.

Table 5. Correlation matrix between CAI. minerals and EQC.

	Cerchar (CAI)	Plagioclase (%)	Clinopiroxene (%)	Amphibole (%)	Iron ore (%)	Cryptocrystalline material (%)
Plagioclase (mm)	0.87					
Plagioclase (%)	0.83	1				
Clinopiroxene (mm)	0.14					
Clinopiroxene (%)	-0.78	-0.96	1			
Amphibole (mm)	-0.07					
Amphibole (%)	-0.11	0	-0.15	1		
Iron ore (%)	0.29	0.2	-0.27	0.15	1	
Cryptocrystalline material (%)	0.04	0.11	-0.33	-0.01	0.07	1
EQC (%)	0.40	0.42	-0.14	-0.41	-0.19	-0.69

A simple linear regression was carried out between *CAI* and the every chemical compound / petrographical property. Those regressions may be mathematically transcribed as:

$$CAI = \alpha \cdot X_i + \beta \tag{2}$$

where X_i indicates the chemical compound / petrographical property (e.g. SiO_2, FeO, Plagioclase content, Amphibole grain size) and α and β are the linear regression coefficients (being the former the slope and the latter the intercept) which are listed in **Table 6**. Besides, that table contains, for each analysis, the coefficient of determination (R^2) as well as the residuals *p-value* (probability value). Assuming 5% as significance level (as is commonly accepted), results with a *p-value* lower than 0.05 might be considered to be statistically significant at a confidence level of 95%.

The higher correlation between *CAI* and chemical compounds were found for SiO_2 (coefficient of determination of 88.3%) and Al_2O_3 (66.8%). **Fig. 5** displays graphically these relations. It should be noted that according to *p-values* chemical compounds TiO_2, MnO, MgO, Na_2O and P_2O_5 appear not to be statistically significant (even though, in the case of P_2O_5 coefficient of determination is considerable higher compared to the other mentioned compounds). Results obtained could be compared with what was recently reported by Er and Tugrul (2016b), who studied the influence of chemical compounds on *CAI* for the granitic rocks of Turkey. Those authors found that SiO_2, Al_2O_3 and Fe_2O_3 were the compounds which presented the highest correlation with CAI, reaching a R^2

value of around a 42%, a similar value to that obtained here for Fe_2O_3, but rather lower for SiO_2 and Al_2O_3 when compared with the results presented on this paper. This difference may be put down to the actual modal difference existing between granitic and andesitic rocks.

Table 6. Simple linear regression results.

	α	β	R^2	p-value
Chemical compounds				
SiO_2	0.0448	-0.0886	0.883	0.000
TiO_2	0.1159	2.2972	0.012	0.349
Al_2O_3	-0.0749	3.5651	0.668	0.000
Fe_2O_3	-0.1328	2.9382	0.481	0.000
FeO	-0.0261	2.5209	0.082	0.014
MnO	-0.0822	2.4444	0.041	0.087
MgO	0.0316	2.2947	0.013	0.337
CaO	-0.0225	2.6019	0.090	0.010
Na_2O	-0.0271	2.4853	0.039	0.090
K_2O	0.0516	2.2742	0.072	0.022
P_2O_5	0.5879	2.2802	0.499	0.552
Modal compounds				
Plagioclase	0.0305	0.6360	0.688	0.000
Clinopyroxene	-0.0261	3.1319	0.604	0.000
Amphibole	-0.0242	2.4696	0.013	0.332
Iron Ore	0.0981	2.3422	0.082	0.014
Cryptocrystalline material	0.0062	2.3258	0.002	0.728
EQC (%)	0.2839	-5.9884	0.169	0.000
Grain size				
Plagioclase	1.8243	0.4447	0.875	0.000
Clinopyroxene	0.1607	2.3067	0.020	0.232
Amphibole	-0.0863	2.4327	0.005	0.553

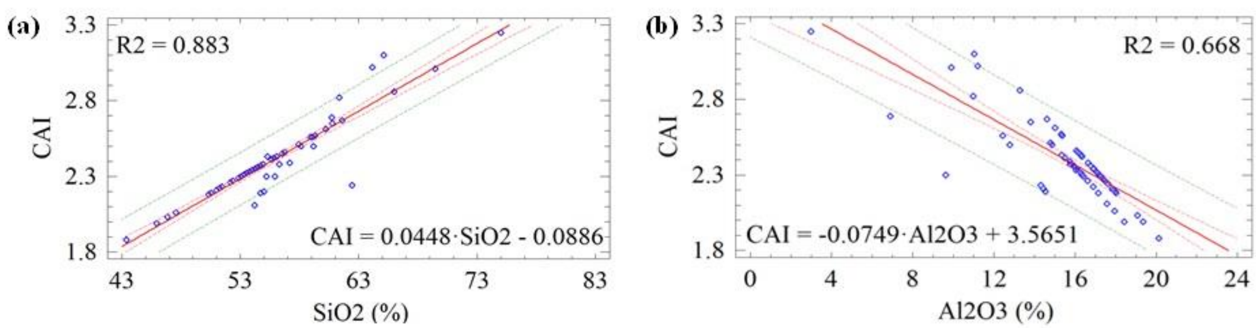

Fig. 5. Simple linear correlation on chemical compounds: a) relation between CAI and SiO2; b) relation between CAI and Al2O3. Red and green dotted line indicate confidence interval and prediction interval, respectively, for a 95% level of significance.

Regarding petrographical properties (modal compounds and grain size), the higher correlation were found for grain size - plagioclase (coefficient of determination of 87.5%) and modal compound - plagioclase (68.8%). **Fig. 6** displays graphically these relations. According to p-values, minerals amphibole and cryptocrystalline material appear not to be statistically significant in terms of modal compound and minerals clinopyroxene and amphibole appear not to be statistically significant in terms of grain size. If results are compared with those obtained by Er and Tugrul (2016b), who also studied the influence of petrographical properties on *CAI*, no match is observed in this case. Granitic rocks studied by those authors had Quartz as the main modal compound, and correlation between *CAI* and *EQC* produced a R^2 value of around 64%, which is rather higher that what was obtained for the andesitic rocks studied in this paper (16.9%). In this case, it is clear that the difference in the petrographical nature between granitic and andesitic rocks is the reason of such discrepancy in results. On the other hand, results obtained are in accordance with Alber (2008) who also established that there was no significant correlation between *CAI* and *EQC*.

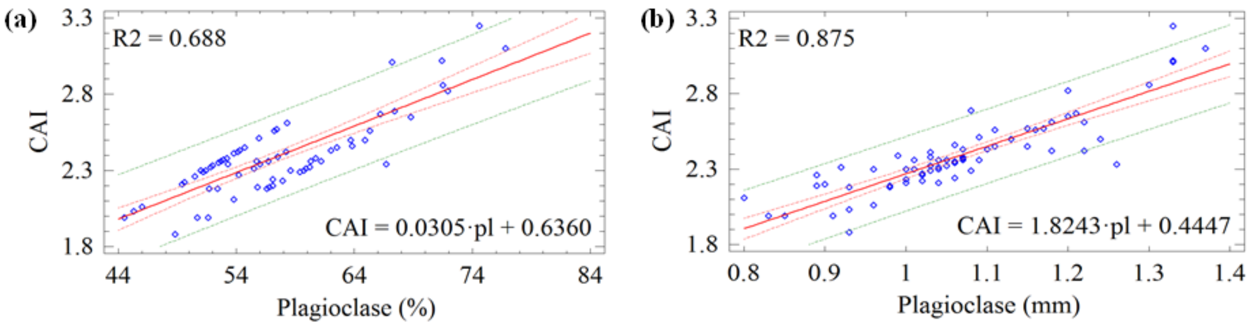

Fig. 6. Simple linear correlation on petrographical properties: a) relation between CAI and modal compound - plagioclase; b) relation between CAI and grain size – plagioclase. Red and green dotted line indicate confidence interval and prediction interval, respectively, for a 95% level of significance.

With the aim of improving correlation, a linear multiregression analysis was conducted. Following that, *CAI* may be expressed as:

$$CAI = \sum \alpha_i \cdot X_i + \beta^* \qquad (3)$$

where X_i indicates the chemical compound / petrographical property (e.g. SiO_2, FeO, Plagioclase content, Amphibole grain size) and α_i and β^* are the linear regression coefficients (being the former the slope for each compound/property and the latter the intercept) which are listed in **Table 7**. Besides, that table contains, for each analysis, the coefficient of determination (R^2) as well as the compound/property *p-value*. Assuming 5% as significance level (as is commonly accepted), results with a *p-value* lower than 0.05 might be considered to be statistically significant at a confidence level of 95%. Those compounds/properties that produced a *p-value* higher than 0.05 were removed from the analysis, since those compounds/properties may be considered not to be statistically significant.

Table 7. Multiregressions results.

	α_i	β^*	R^2	p-value
Chemical compounds				
SiO_2	0.0552	-1.3191	0.924	0.000
TiO_2	-			-
Al_2O_3	-			-
Fe_2O_3	-			-
FeO	0.0261			0.000
MnO	-			-
MgO	0.0545			0.000
CaO	0.0244			0.000
Na_2O	0.0223			0.000
K_2O	0.0223			0.000
P_2O_5	-			0.004
Modal compounds				
Plagioclase	0.0305	0.6360	0.688	0.000
Clinopyroxene	-			-
Amphibole	-			-
Iron Ore	-			-
Cryptocrystalline material	-			-
Grain size				
Plagioclase	1.8243	0.4447	0.875	0.000
Clinopyroxene	-			-
Amphibole	-			-

When comparing results obtained using multiregression analysis with simple regression, it may be observed that the use of multiregression slightly improves the estimation of *CAI* based on chemical compounds. Coefficient of determination increases from 88.3% (best result obtained for simple regression for SiO_2) to 92.4%, and in the correlation equation take part SiO_2, FeO, MgO, CaO, Na_2O and K_2O compounds:

$$CAI = 0.055 \cdot SiO_2 + 0.026 \cdot FeO + 0.055 \cdot MgO + 0.024 \cdot CaO + 0.022 \cdot Na_2O + 0.022 \cdot K_2O - 1.32 \qquad (4)$$

It is interesting to note that Al_2O_3 resulted not to be statistically significant in this analysis, even though that compound reached the second highest R^2 when performing the simple regression analyses.

For the case of petrographical properties, every property except plagioclase (as modal compound and as grain size) showed not to be statistically significant. Therefore, no improvement was achieved by using multiregression analysis (note that values for α_i, β^* and R^2 are exactly the same as those obtained with a simple linear regression for plagioclase).

Eventually, if a graph comparing *CAI* vs. the modal compounds of the plagioclase and vs. the rest of the compounds (clinopyroxene, amphibole and cryptocrystalline material) is made (**Fig. 7**), the regression analyses conducted are confirmed. The correlation of *CAI* with plagioclase is positive so the more of this compound, the higher the value of *CAI*. On the other hand, the content of the other compounds tend to lower the *CAI*, as was noted in the statistical summary of the results.

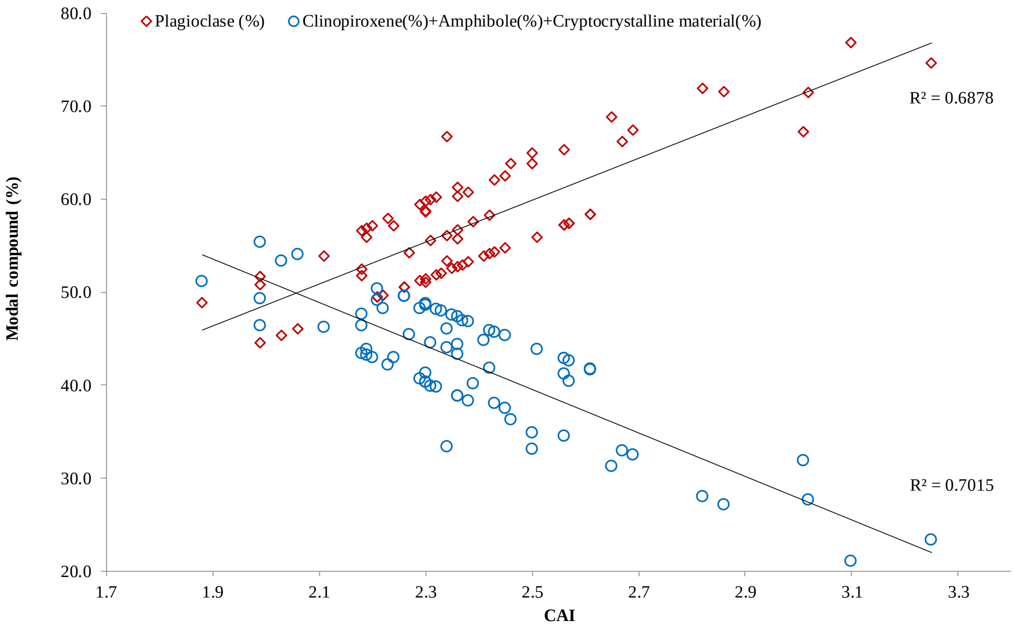

Fig. 7. Graph comparing CAI vs. the modal compounds of the plagioclase and vs. the rest of the compounds (clinopyroxene, amphibole and cryptocrystalline material).

6. Conclusion

Relation between Cerchar Abrasivity Index (*CAI*) and the chemical compounds and petrographical properties (modal compounds and grain size) of a series of andesitic rocks samples coming from the central area of Ecuador was investigated. A total of 73 andesitic samples were subjected to XRF analyses to find their chemical compounds. Modal compounds and minerals grain size were obtained by preparing thin sections of each sample. *CAI* was computed by conducting a Cerchar abrasivity test on each sample. Density, uniaxial compression strength and tensile strength of the andesitic rock was also obtained to complete the geotechnical characterization of that material. Several regression analyses were performed with the aim of establishing the significance and relation that the different chemical compounds, the modal compounds and the minerals grain size might have on *CAI*.

From the results obtained it may be concluded:

a) The andesitic samples resulted to be composed of mainly plagioclase (nearly 60%), with some content in clinopyroxenes (around 30%) and some traces of amphibole and iron ore. Chemically, the samples mainly consist of SiO_2 (ca. 50%) with some content in Al_2O_3 and CaO, and traces of other compounds such as Fe_2O_3, MgO and P_2O_5. Regarding physical and mechanical properties, density of andesitic rock samples was found to be about 25 kN/m^3, uniaxial compression strength 177 MPa and tensile strength 9 MPa. *CAI* achieved an average value of 2.39.

b) The Cerchar tests showed that there is about 30% chance of scratching amphiboles and clinopyroxenes, approximately 60% of plagioclase and 10% of matrix, and this agree with the distribution of minerals in the thin sections.

c) The correlation matrix between *CAI*, minerals and EQC shows that the *CAI* values with the plagioclase are logical in content and size of the crystal. Also with amphibole, but it does not have seemingly sense the variation that the clinopiroxeno presents. However, although the value of the correlation coefficient (0.78) is low, the most significant is the negative sign. This indicates that the greater existence of clinopyroxene lower *CAI*.

d) A strong linear correlation was found between *CAI* and SiO_2 (R^2 equal to 88.3%), as well as between *CAI* and plagioclase grain size (R^2 equal to 87.5%).

e) A no clear relation was found between *CAI* and *EQC* (Equivalent Quartz Content).

f) Relation between *CAI* and plagioclase content was found not to be strong (R^2 equal to 68.8%). Similarly, correlation between *CAI* and Al_2O_3 or Fe_2O_3 was also rather weak (R^2 equal to 66.8% and 48.1%, respectively). Especially, it is interesting to mention that the two oxides were found not to be statistically significant when performing a multiregression analysis between *CAI* and chemical compounds.

g) An estimation of *CAI* for the andesitic rocks of central Ecuador may be performed using the linear regressions obtained in this paper for plagioclase grain size and/or the content in SiO_2, FeO, MgO, CaO, Na_2O and K_2O compounds (multiregression). The use of those relations will enable an easy and fast estimation of *CAI* without the necessity of performing any Cerchar abrasivity test.

h) Comparison of *CAI* vs. the modal compounds of the plagioclase and *CAI* vs. the rest of the compounds shows that while plagioclase results in a clear positive influence on *CAI*, the content of the other compounds tend to lower the index.

Acknowledgements

This research did not receive any specific grant from funding agencies in the public, commercial, or not-for-profit sectors.

References

NF P 94-430-1, 2000. Determination du pouvoir abrasif d'une roche— Partie 1: Essai de rayure avec une pointe. Association française de Normalisation (AFNOR), Paris.

Al-Ameen, S.L., Waller, M.D., 1994. The influence of rock strength and abrasive mineral content on the CERCHAR abrasive index. Eng. Geol. 36, 293–301.

Alber, M., 2007. Stress dependency of the Cerchar Abrasivity Index (CAI) and its effects on wear of selected rock cutting tools. Tunn. Undergr. Space Technol. 9, 351–539.

Alber, M., 2008. Stress dependency of the Cerchar abrasivity index (CAI) and its effects on wear of selected rock cutting tools. Tunn. Undergr. Space Technol. 23, 351–359.

Alber, M., Yaralı, O., Dahl, F., Bruland, A., Käsling, H., Michalakopoulos, T.N., Cardu, M., Hagan, P., Aydın, H, Özarslan, A., 2014. ISRM suggested method for determining the abrasivity of rock by the CERCHAR abrasivity test. Rock Mech. Rock Eng. 47, 261–266.

ASTM D3967, 2001. Standard test method for splitting tensile strength of intact rock core specimens. American Society for Testing and Materials, West Conshohocken, PA.

ASTM D7012, 2010. Standard test method for compressive strength and elastic module of intact rock core specimens under varying states of stress and temperatures. American Society for Testing and Materials, West Conshohocken, PA.

ASTM D7625, 2010. Standard Test Method for Laboratory Determination of Abrasiveness of Rock Using the CERCHAR Method. American Society for Testing and Materials, West Conshohocken, PA.

Atkinson, T., Cassapi, V.B., Singh, R.N., 1986a. Assessment of abrasive wear resistance potential in rock excavation machinery. Int. J. Min. Geol. Eng. 3, 151–163.

Atkinson, T., Denby, B., Cassapi, V.B., 1986b. Problems associated with rock material properties in surface mining equipment selection. Trans. Inst. Min. Metall. Section. A Miner. Ind. 95, A80–A86.

Boland, M.P., Pilatasig, L.F., Ibandango, C.E., McCourt, W.J., Aspden, J.A., Hughes, R.A., Beate B., 2000. Geology of the Western Cordillera between 0°-1°N, Mining Development and

Environmental Control Project, Map and Geological Information Program, Report No. 10, (Proyecto de Desarrollo Minero y Control Ambiental, Programa de Informacion cartografica y Geológica, Informe No. 10), CODIGEM-BGS, Quito, Ecuador, pp 72. In Spanish.

CERCHAR, 1986. The CERCHAR abrasiveness index. Centre d'Etudes et des Recherches des Charbonages de France, Verneuil, France.

Deliormanlı, A., 2011. Cerchar abrasivitiy index (CAI) and its relation to strength and abrasion test methods for marble stones. Constr. Building Mat. 30, 16–21.

Deliormanlı, A.H., 2012. Cerchar abrasivity index (CAI) and its relation to strength and abrasion test methods for marble stones. Constr. Build Mater. 30, 16–21.

Er, S., Tugrul, A., 2016a. Correlation of physico-mechanical properties of granitic rocks with Cerchar Abrasivity Index in Turkey. Measurement 91, 114–123.

Er, S., Tugrul, A., 2016b. Estimation of Cerchar abrasivity index of granitic rocks in Turkey by geological properties using regression analysis. B. Eng. Geol. Environ. 75(3), 1325–1339.

Fowell, R.J., Abu Bakar, M.Z., 2007. A review of the Cerchar and LCPC rock abrasivity measurement methods. Proceeding of the 11th Congress of the International Society for Rock Mechanics 155–160.

Hamzaban, M.T., Memarian, H., Rostami, J., 2014. Continuous monitoring of pin tip wear and penetration into rock surface using a new Cerchar abrasivity testing device. Rock Mech. Rock Eng. 47(2), 689–701.

Hamzaban, M.T., Memarian, H., Rostami, J., Ghasemi-Monfared, H., 2014. Study of rock-pin interaction in Cerchar abrasivity test. Int. J. Rock Mech. Min. Sci. 72, 100–108.

ISRM, 2007. The Complete ISRM suggested methods for rock characterization, testing and monitoring: 1974–2006. International Society for Rock Mechanics, Lisbon.

Kahraman, S., Alber, M., Fener, M., Gunaydin, O., 2010. The usability of Cerchar abrasivity index for the prediction of UCS and E of Misis Fault Breccia: regression and artificial neural networks analysis. Expert Syst. Appl. 37, 8750–8756.

Käsling, H., Thuro, K., 2010. Determining abrasivity of rock in the laboratory. European Rock Mechanics Symposium. EUROCK 2010, Laussane, Switzerland.

Lassnig, K., Latal, C., Klima, K., 2008. Impact of grain size on the Cerchar abrasiveness test. Ernst and Sohn Verlag für Architektur und technische Wissenschaften GmbH and Co. KG. Berlin Geomechanik und Tunnelbau 1, Heft 1.

Majeed. Y., Abu Bakar, M.Z., 2016. Statistical evaluation of CERCHAR Abrasivity Index (CAI) measurement methods and dependence on petrographic and mechanical properties of selected rocks of Pakistan. Bull. Eng. Geol. Environ. 75, 1341–1360.

Michalakopoulos, T.N., Anagnostou, V.G., Bassanou, M.E., Panagiotou, G.N., 2005. The influence of steel styli hardness on the Cerchar abrasiveness index value. Inter. J. Rock Mech. Mining. Sci. Geomechan. Abstracts 43, 321–327.

Moradizadeh, M., Ghafoori, M., Lashkaripour, G.R., Tarigh Azali, S., 2013. Utilizing geological properties for predicting cerchar abrasiveness index (CAI) in sandstones. Int. J. Emerg. Technol. Advan. Eng. 3(9), 99–109.

Plinninger, R., Kasling, H., Thuro, K., Spaun, G., 2003. Testing conditions and geomechanical properties in influencing the CERCHAR abrasiveness index (CAI) value. J. Rock Mech. Mining Sci. 40, 159–263.

Rostami, J., Ghasemi, A., Gharahbagh, A.E., Dogruoz, C., Dahl, F., 2014. Study of dominant factors affecting cerchar abrasivity index. Mech. Rock Eng. 47, 1905–1919.

StatPoint Technologies, Inc., 2009. STATGRAPHICS Centurion XVI User Manual. The Plains, VA.

Suana, M., Peters, T., 1982. The CERCHAR abrasivity index and its relation to rock mineralogy and petrography. Rock Mech. Rock Eng. 15, 1–7.

Thuro, K., 1997. Prediction of drillability in hard rock tunneling by drilling and blasting, in: Golser, Hinkel and Schubert (Eds.), Tunnels for People, Balkema, Rotterdam, pp. 103-108.

Vallejo, C., 2007. Evolution of the Western Cordillera in the Andes of Ecuador (Late Cretaceous–Paleogene). PhD. Dissertation, Institute of Geology, ETH Zürich.

Vallejo, C., Winkler, W., Spikings, R.A., Luzieux, L., Heller, F., Bussy, F., 2009. Mode and timing of terrane accretion in the forearc of the Andes in Ecuador, in: Kay, S.M., Ramos, V.A., Dickinson, W.R. (Eds.), Backbone of the Americas: Shallow Subduction, Plateau Uplift, and Ridge and Terrane Collision, Geol. Soc. Am. Mem. 204.

Vera, R.H., 2016. Geology of Ecuador. Iberia, Quito.

Vezzoli, L., Apuani, T., Corazzato, C., Uttini, A., 2017. Geological and geotechnical characterization of the debris avalanche and pyroclastic deposits of Cotopaxi Volcano (Ecuador). A contribute to instability-related hazard studies. J. Volcanol. Geotherm. Res. 332, 51–70.

West, G., 1989. Rock abrasiveness testing for tunneling. Int. J. Rock Mech. Min. Sci. Geomech. Abstr. 26, 151–160.

Yarali, O., Yasar, E., Bacak, G., Ranjith, P.G., 2008. A study of rock abrasivity and tool wear in coal measures rocks. Int. J. Coal Geol. 74, 53–66.